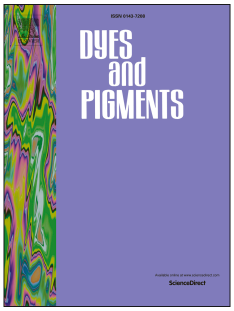

Yellow emitting materials: Truxene-based conjugated hyperbranched polymer containing difluoroboron-diketonate complexes

Xin Wen, Dongxin Zhang, Tianci Ren, Jinchong Xiao, Yonggang Wu, Libin Bai, Xinwu Ba

PII: S0143-7208(16)31051-8
DOI: 10.1016/j.dyepig.2016.10.037
Reference: DYPI 5553

To appear in: *Dyes and Pigments*

Received Date: 29 July 2016
Revised Date: 24 October 2016
Accepted Date: 25 October 2016

Please cite this article as: Wen X, Zhang D, Ren T, Xiao J, Wu Y, Bai L, Ba X, Yellow emitting materials: Truxene-based conjugated hyperbranched polymer containing difluoroboron-diketonate complexes, *Dyes and Pigments* (2016), doi: 10.1016/j.dyepig.2016.10.037.

Table of Contents

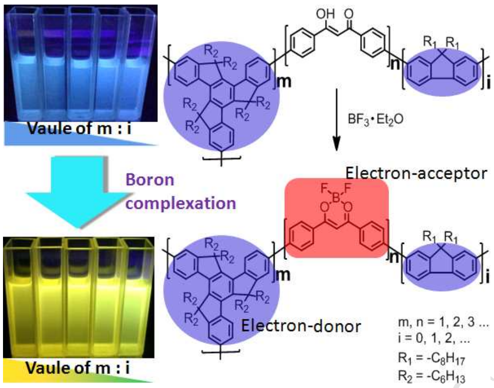

Yellow Emitting Materials: Truxene-Based Conjugated Hyperbranched Polymer Containing Difluoroboron-Diketonate Complexes[a]

Xin Wen, Dongxin Zhang, Tianci Ren, Jinchong Xiao, Yonggang Wu, Libin Bai, Xinwu Ba**

College of Chemistry and Environmental Science, Hebei University, Baoding 071002, China

Abstract

A series of novel hyperbranched polymers **BF_2-HP**(**1-4**) containing difluoroboron-diketonate complexes and truxene units have been synthesized. To achieve the target polymers, the precursors **Boc-HP**(**1-4**) were obtained through the Pd(0)-catalyzed Suzuki polymerization with an “A_2 + B_3” or “A_2 + B_2 + B_3” approach in different molar ratios. After the deprotection of Boc-groups, the reaction with BF_3 gave the polymers **BF_2-HP(1-4)**. The new BF_2 containing polymers exhibited red-shifts in their UV-vis absorption and emission compared with their uncomplexed counterparts. The tunable hyperbranched architectures of **BF_2-HP**(**1-4**) resulted in diverse optical properties. With the decrease of linear units in **BF_2-HP**(**1-4**), the emission peaks in chloroform solution presented a significant blue-shift, whereas a red-shift was noted in films. Notably, the hyperbranched architectures could suppress the aggregation more effectively than the linear architectures not only in poor solvents such as DMF but also in the film states. In addition, these polymers showed high thermal stability, and good solubility in common organic solvents.

Keywords: Hyperbranched polymers; Difluoroboron-diketonate complexes; Optoelectronic property; Truxene units; Suzuki polycondensation.

*****Corresponding author. Tel./fax: +86-312-5079317.

E-mail address: zhonggou556@hbu.edu.cn (L. Bai); baxw@hbu.edu.cn (X. Ba).

Postal address: No.180 Wusi East Road, Baoding City, 071002, Hebei, P.R.China

1. Introduction

Organoboron π-conjugated polymers have attracted much interest in the last few decades because of their unique electronic and optical properties [1-7]. Difluoroboron (BF_2) β-diketonate π-conjugated systems are fascinating subunits for fabricating emissive and electronic polymers, due to their large molar absorption coefficient, high luminescence quantum yield and room-temperature phosphorescence [8,9]. Several efforts have been devoted to the design and synthesis of polymers containing difluoroboron β-diketonate units [10-14]. For instance, Fraser et al. found that polycaprolactones containing difluoroboron β-diketonate units exhibited intense blue fluorescence upon UV excitation and blue-shifted emission [15]. More recently, Chujo et al. have reported the optical properties of conjugated polymers which can be effectively tuned by the ratios of difluoroboron β-diketonate units in the main chain of polymers [16]. However, for π-conjugated polymers, their optical properties strongly depended on the molecular structure and inter- or intra-molecular interactions [17-20]. In particular, concentration-quenching often occurred because of the non-specific aggregation of π-conjugated polymers. Therefore, the suppression of intra- and inter- molecular π-π stacking in the solid state seemed to be important to overcome this problem.

Hyperbranched polymers have been widely used in many fields due to their three-dimensional dentritic architectures, a high number of the terminal groups, as well as little chain entanglement [21-25]. Using the unique feature of hyperbranched polymers, the aggregation of π-conjugated polymers may be effectively suppressed, which is beneficial for a higher light emitting efficiency. On the base of this view, various kinds of π-conjugated hyperbranched polymers were synthesized and used as active layers in optical materials such as polymer-based organic light emitting diodes (OLEDs), field effect transistors, solar cells and biosensors [26-30]. The concept in our work is to construct novel difluoroboron β-diketonate-containing hyperbranched conjugated polymers with diverse optoelectronic properties, which might improve the performance of organic materials in the application for OLED devices.

In continuation of our previous work [31,32], we synthesized BF_2-complexed hyperbranched polymers **BF_2-HP(1-4)** with different molar ratios of BF_2-diketonate complexes and truxene units (Scheme 1). The tunable hyperbranched architectures of **BF_2-HP(1-4)** resulted in diverse optical properties. As expected, the results showed that the hyperbranched architecture effectively suppress the aggregation and hyperbranched polymers **BF_2-HP(1-4)** emitted strong yellow light not only in organic solvents, but also in poor solvent or in film. Additionally, thermal gravimetric analysis (TGA) displays that they all exhibit good thermal stability.

2. Results and Discussion

The synthetic routes to the monomers and polymers are outlined in Scheme 2. **M1** was obtained by the condensation reaction of the commercially available 4-bromoacetophenone and methyl 4-bromobenzoate in the presence of NaH. Introduction of di-*tert*-butyl dicarbonate into **M1** by using 4-*N*,*N*-dimethylaminopyridine (DMAP) as the catalyst can produce **M2**. Monomers **M3** and **M4** were synthesized in our lab according to a published procedure [33,34].

The hyperbranched polymers **Boc-HP1-4** were prepared through Suzuki cross-coupling reaction by using **M2** as A_2, **M3** as B_2 and **M4** as B_3, respectively, and 1-bromobenzene was employed to cap the boron containing end groups (Scheme 2). In the synthesis process, the feed ratio between boronic acid pinacol ester (-B) and -Br was always 1.65 (Table S1). In order to increase the linear length in hyperbranched polymers, the amount of **M2** kept constant while feed ratios between **M3** and **M4** increased (Table S1), affording hyperbranched polymers from **Boc-HP1** to **Boc-HP4**, correspondingly. In the absent of truxene monomer **M4**, linear polymer **Boc-LP5** was obtained. The yields of those polymers were 44%, 63%, 62%, 62% and 53%, respectively. The relative lower yields of **Boc-HP1** and **Boc-LP5** might be ascribed to the gelation formation and the incomplete reaction of **M4**, respectively.

The number-average molecular weights (M_n) of polymers were determined by gel permeation chromatography (GPC) using THF as the eluent and a polystyrene standard (Fig. 1) and the results were listed in Table 1. As shown in Fig. 1a, the M_n of **Boc-HP1-4** and **Boc-LP5** decreased with the increase of linear length from **Boc-HP1** to **Boc-LP5**. When **M1** was used instead of **M2**, the M_n of polymers were much lower, less than 4×10^3 g mol^{-1}, which might be ascribed to the interconversion between the keto and enol [35]. **OH-HP1-4** and **OH-LP5** were obtained in high yields by removing the *O*-Boc groups with piperidine in methylene chloride (Scheme 2). Complex of **OH-HP1-4** and **OH-LP5** with $BF_3 \cdot Et_2O$ gave polymers **BF$_2$-HP1-4** and **BF$_2$-LP5** [16], respectively, and the total yields were in the range of 41% to 59%. After boron complexation, the M_n decreased (Fig. 1b). Furthermore, the M_n and molecular weight distributions (M_w/M_n) of **BF$_2$-HP1-4** and **BF$_2$-LP5** were 2.17-1.21×10^4 g mol^{-1} and 8.01-1.69, respectively (Table 1). (Table 1). It should be noted that these polymers **BF$_2$-HP1-4** and **BF$_2$-LP5** displayed better solubility in common organic solvents such as tetrahydrofuran, methylene chloride, chloroform than that of linear counterparts [16], which might result from the hyperbranched architectures.

The optical properties of the hyperbranched polymers were investigated by UV-Vis absorption (Fig. 2a, c, e) and photoluminescence (PL) spectra (Fig. 2b, d, f) in dilute chloroform solution. **Boc-HP1** presented the absorption peaks at 318 nm and 371 nm (Fig. 2a). Upon the increase of fluorene units in the polymers, **Boc-HP2-4** and **Boc-LP5** displayed the broad absorption bands at 376 nm, 378 nm, 378 nm, 383 nm, while the peak at 318 nm decreased gradually. In comparison, the absorption spectra of **OH-HP1-4** and **OH-LP5** displayed a negligible change relative to their *O*-Boc protected counterparts (Boc-HP 1-4) (Fig. 2c). After complexed with BF_3, however, the BF_2-complex polymers **BF$_2$-HP1-4** and **BF$_2$-LP5** showed an obvious red-shift to 460 nm, and the absorption peaks became broad (Fig. 2e). It might be ascribed to the formation strong push (truxene parts)-pull (BF_2-complex moiety) systems that could lead to intramolecular charge transfer (ICT) state [36,37].

Fig. 2b showed the emission spectra of **Boc-HP1** with the maximum peak at 467 nm. In the case of **Boc-HP2-4** and **Boc-LP5**, the emission peaks blue-shifted to 465 nm, to 464 nm, to 461 nm and 457 nm. **OH-HP1-4** and **OH-LP5** also displayed the same trend, but they emitted strong blue light (Fig. 2d). This might be attributed to the removal of electron-withdrawing units (Boc). The BF_2-complex polymers **BF_2-HP1-4** and **BF_2-LP5** exhibited significant red-shift spectra as shown in Fig. 2f, and these polymers emitted strong yellow light. Clearly, with the increase of linear length in hyperbranched architectures, polymers featured blue-shift emission profile from **BF_2-HP1** to **BF_2-LP5**, which was consistent with the absorption results. It is apparent that the delocalization effect of fluorine units was smaller than that in truxene units, thus the band gap of conjugate system became larger, resulting in a blue-shift from **BF_2-HP1** to **BF_2-LP5.** Furthermore, the quantum yields of **BF_2-HP1-4** and **BF_2-LP5** were measured using *N*,*N′*-bis(1-ethylpropyl)-3,4,9,10-perylene-bis (dicarboximide) as a reference standard at room temperature (Table 2). The Φ_{PL} increased from **BF_2-HP1** to **BF_2-LP5** (Table 2). These result indicated that the concentration of light-emitting units in the internal structure of hyperbranched polymers was higher than the linear one, thus resulting in the fluorescence quenching to some extent [38].

To further confirm the ICT processes of these polymers, the PL spectra in different solvents (CH_2Cl_2, THF and DMF) with different polarity were performed (Table 2). The emission spectra were collected with the excitation light at the peaks determined from the absorption spectra. From $CHCl_3$, to CH_2Cl_2, to DMF, except for THF, all polymers **BF_2-HP1-4** and **BF_2-LP5** showed a marked red-shift by increasing the solvent polarity. In addition, these solvent dependencies were confirmed by the Lippert-Mataga plot [39-41], which showed a linear correlation of the Stokes shift with solvent polarity (Fig. 3). These results were strongly indicative of ICT. We note that, in the case of THF as the solvent, irregular Stokes shifts were observed which were lower than estimated. Exactly why this should be so is not absolutely clear to us but we suggest that this was either related to the good dissolution of the polymers in THF or their hyperbranched structure. The same tendency has also been observed in the data reported by other groups [16,42].

The spectra of **BF_2-HP1-4** and **BF_2-LP5** thin films prepared on quartz plates were measured (Fig. 4) and these results and their quantum yields were shown in Table 3. The absorption and emission peaks featured a red-shift emission profile from **BF_2-HP1** to **BF_2-LP5**, providing an opposite trend compared with those of polymers in chloroform. In general, the three-dimensional architecture could suppress π-π stacking in hyperbranched polymers compared to their linear counterpart, and thus the intermolecular stacking increased along with the decrease of the degree of branching from **BF_2-HP1-4** to **BF_2-LP5,** accounting for the red-shift for polymers in film states. As can be seen from Table 3, a 19 nm red-shift was observed from **BF_2-HP1** to **BF_2-LP5**. Notably, the emission peak of **BF_2-HP1** in chloroform was almost the same as that of in film; whereas the emission peak of **BF_2-LP5** displayed a 45 nm red-shift from chloroform solution to film state. Taking the absorption and emission spectra into consideration, one does believe that the hyperbranched architectures could suppress the aggregation more effectively than the linear ones in the film state, consistent with the trend in a poor solvent such as DMF.

The electrochemical properties of the hyperbranched polymers **BF_2-HP1-4** and **BF_2-LP5** was recorded using cyclic voltammetry (CV), which was conducted in anhydrous methylene chloride using tetrabutylammonium hexafluorophosphate ($TBAPF_6$) as a supporting electrolyte with a standard three-electrode electrochemical cell containing a Pt counter electrode, Ag/Ag^+ as the reference electrode, and a glass carbon working electrode. Fig. 5 shows the cyclic voltammograms of **BF_2-HP1-4** and **BF_2-LP5** at a scan rate of 30 mV s^{-1} in the range of 0-1.7 V. The HOMO energy levels were calculated according to the following equation: HOMO = $-([E_{onset}]^{ox} + 4.4)$ eV. The band gap (ΔE) of polymers **BF_2-HP1-4** and **BF_2-LP5** were calculated from the UV-vis absorption onset of the polymers. The LUMO levels were obtained on the basis of the equation: $E_{LUMO} = E_{HOMO} + E_{gap}$.

The results are summarized in Table 4. With the increase in the linear length of hyperbranched polymer, HOMO energy levels were more negative, and the band gap became larger.

The thermal properties of the polymers **BF_2-HP1-4** and **BF_2-LP5** were further investigated by thermogravimetric analysis (TGA) in a nitrogen atmosphere. As shown in Fig. 6, the onset temperatures of 5% weight loss of these polymers were 221 °C, 223 °C, 201 °C, 226 °C, and 210 °C, respectively, indicating that the polymers **BF_2-HP1-4** and **BF_2-LP5** have good thermal stability.

3. Experimental Section

3.1 General

Chemical reactants were purchased from Soochiral Chemical Science & Technology Co., Ltd. and *J&K* Scientific Ltd. and used without further purification. Organic solvents were rigorously purified and dried by standard methods.

The reactions were monitored by TLC with silica gel 60 F254 (Merck, 0.2 mm). Column chromatography was carried out on silica gel (200-300 mesh). The ^{1}H NMR and ^{13}C NMR spectra were measured with a 600 MHz Bruker spectrometer using tetramethylsilane as reference at 298 K. High-resolution mass spectra (HRMS) were recorded on a Bruker solariX FTICR mass spectrometer operating in a MALDI mode. Fourier transform infrared spectroscopy (FTIR) was tested on a Varian-640 spectrophotometer (KBr pellet technique). The M_n and weight-average molecular weight (M_w) were assessed using a Waters 2414 GPC equipped with Waters HT4 and HT3 column-assembly and a Waters 2414 refractive index detector (eluent, THF; flow rate, 1.00 mL min^{-1}), which is calibrated by the polystyrene standard (the M_n of polystyrene standard are 3790, 13000, 30300, 52000, 219000 g mol^{-1}). UV-vis and fluorescence spectra were carried out on Shimadzu UV-2550 and RF5300PC spectrophotometer, respectively. Absolute fluorescence quantum yields of polymers in film ($\Phi_{\mathrm{PL,\ film}}$) were measured on Edinburgh FLS920 steady fluorimeter with a calibrated integrating sphere (excited at 365 nm). The cyclic voltammetry measurement was performed on CHI

630A electrochemical analyzer at room temperature at atmospheric pressure in anhydrous methylene chloride with a scanning rate of 30 mV s^{-1}, having tetrabutylammonium hexafluorophosphate ($TBAPF_6$) as a supporting electrolyte using a standard three-electrode electrochemical cell containing a Pt counter electrode, acetonitrile Ag/Ag^+ (0.01 M in CH_3CN) as the reference electrode, and a glassy carbon working electrode. The system was calibrated with the standard ferrocene/ferrocenium (Fc) redox system and assumption that the energy level of Fc is 4.8 eV below vacuum. TGA measurements were carried out Pyris 1 TGA under a nitrogen atmosphere (20 mL min^{-1}) at a heating rate of 20 °C min^{-1}.

3.2 Synthesis of Monomers and Polymers

M1. In a 250-mL three-necked flask with a dropping funnel, a mixture of 4-bromoacetophenone (2.40 g, 12 mmol) and NaH (0.96 g, 28 mmol) in dry THF (40 mL) was placed under an argon atmosphere. The dry THF solution (20 mL) containing methyl 4-bromobenzoate (2.84 g, 13.2 mmol) was added dropwise at 5 °C in an ice bath within 15 min, and the mixture was further stirred for 8 h at 50 °C. The reaction mixture was allowed to cool down to room temperature, and 10% HCl was then gently added until the solution color gradually turned from orange to light yellow. Water (50 mL) and ethyl acetate (200 mL) were added, and the organic layer was separated and dried over anhydrous Na_2SO_4. After removing a large portion of the ethyl acetate under reduced pressure, crystallisation form the hot ethyl acetate gave a plate-like crystal of 1,3-bis(4-bromophenyl)-propane-1,3-dione (2.84 g, 62%). ^1H NMR (600MHz, DMSO-d_6, δ): 16.98 (s, 1H), 7.34 (s, 1H), 8.11 (d, J = 7.2 Hz, 4H), 7.85 (d, J = 7.8 Hz, 4H). ^{13}C NMR (150MHz, d_6-DMSO, δ): 184.8, 134.1, 132.4, 131.0, 129.9, 127.6, 94.0. FTIR (KBr, cm^{-1}): 3468, 1920, 1579, 1511, 1477, 1294, 1068, 1000, 775. HRMS (MALDI-TOF): Calcd. for $C_{15}H_{11}Br_2O_2$: m/z 382.9105, found: $[M+H]^+$ 382.9101.

M2. A mixture of **M1** (2.0 g, 5.2 mmol), di-*tert*-butyl dicarbonate (5.71 g, 26.2 mmol) and DMAP (63.4 mg, 0.52mmol) in dry THF (80 mL) was stirred at 45 °C for 10 h under an argon atmosphere.

After cooling to room temperature, the solvent was removed under reduced pressure, and recrystallization from CH_2Cl_2 and hexane afforded **M2** as a yellowish crystal (1.35 g, 54%). ^1H NMR (600MHz, DMSO-d_6, δ): 7.83 (d, J = 8.4 Hz, 2H), 7.62 (d, J = 8.4 Hz, 2H), 7.58 (s, 1H), 7.09 (s, 1H), 1.55 (s, 9H). ^{13}C NMR (150MHz, DMSO-d_6, δ): 182.4, 151.5, 144.9, 132.5, 128.1, 127.5, 127.2, 125.0, 123.4, 122.9, 121.1, 104.7, 79.8, 22.9. FTIR (KBr, cm^{-1}): 3072, 2981, 1907, 1745, 1664, 1600, 1481, 1301, 1238, 1145, 1079, 1002, 817. HRMS (MALDI-TOF): Calcd. for $C_{20}H_{18}Br_2O_4Na$: m/z 504.9449, found: $[M+Na]^+$ 504.9445.

Boc-HP1-4 and **Boc-LP5.** A mixture of the corresponding monomers and $NaHCO_3$ was added to a solution of THF (20 mL) and H_2O (4 mL). Reaction system was carefully degassed and then $Pd(PPh_3)_4$ (3 mg) was added. The reaction mixture was heated at 80 °C with vigorous stirring for 48 h under an argon atmosphere. Bromobenzene (100 mg, 0.64 mmol) was added to end-cap the boron containing end groups. After refluxing for another 12 h, the mixture was cooled to room temperature. Then water (50 mL) and CH_2Cl_2 (200 mL) were added, the organic layer was separated and dried over anhydrous Na_2SO_4. After removal of most of the solvent, the resulting mixtures were precipitated in methanol. The crude products were repurified by precipitation from THF into a large excess of hexane again and dried under vacuum to give yellow polymers.

Boc-HP1: ^1H NMR (600MHz, DMSO-d_6, δ): 8.75-8.31 (br, 3H), 8.3-8.05 (br, 4H), 8.05-7.38 (br, 19H), 3.01-2.88 (br, 6H), 2.31-1.98 (br, 9H), 1.48 (s, 9H), 1.02-0.67 (br, 58H). GPC: M_w = 56300; M_n = 28300; polydispersity = 1.99.

Boc-HP2: ^1H NMR (600MHz, DMSO-d_6, δ): 8.74-8.32 (br, 3H), 8.32-8.05 (br, 4H), 8.04-7.57 (br, 17H), 3.31-2.76 (br, 6H), 2.40-1.97 (br, 9H), 1.48 (s, 10H), 1.05-0.68 (br, 55H). GPC: M_w = 69400; M_n = 28100; polydispersity = 2.47.

Boc-HP3: ^1H NMR (600MHz, DMSO-d_6, δ): 8.63-8.32 (br, 3H), 8.32-8.06 (br, 5H), 8.05-7.57 (br, 30H), 3.30-2.75 (br, 6H), 2.31-1.94 (br, 12H), 1.48 (s, 9H), 1.02-0.69 (br, 54H). GPC: M_w = 60800; M_n = 26700; polydispersity = 2.28.

Boc-HP4: ^{1}H NMR (600MHz, DMSO-d_6, δ): 8.63-8.34 (br, 3H), 8.29-8.04 (br, 14H), 8.03-7.47 (br, 81H), 3.33-2.76 (br, 6H), 2.46-1.83 (br, 6H), 1.48 (s, 9H), 1.02-0.69 (br, 60H). GPC: M_w = 44100; M_n = 21200; polydispersity = 2.08.

Boc-LP5: ^{1}H NMR (600MHz, DMSO-d_6, δ): 8.20-8.11 (br, 4H), 7.95-7.47 (br, 10H), 7.01 (br, 1H), 2.17-1.98 (br, 10H), 1.43 (br, 9H), 1.35-1.16 (br, 10H), 0.94-0.54 (br, 18H). GPC: M_w = 30200; M_n = 15100; polydispersity = 2.00.

OH-HP1-4 and **OH-LP5.** Piperidine (3.00 μL, 0.3 mmol) was added to a solution of **Boc-HP1-4** or **Boc-LP5** (100 mg) in CH_2Cl_2 (20 mL). After stirring for 24 h at room temperature, water and CH_2Cl_2 (100 mL) were added. The organic layer was separated and washed with water three times, dried over Na_2SO_4, and concentrated to dryness. The crude polymer was purified by precipitation from THF into hexane and dried under vacuum to give yellow polymers.

OH-HP1: ^{1}H NMR (600MHz, DMSO-d_6, δ): 17.25 (br, 1H), 8.60-8.30 (br, 3H), 8.29-8.16 (br, 3H), 8.03-7.59 (br, 12H), 7.06 (br, 1H), 3.11-2.93 (br, 6H), 2.30-2.00 (br, 12H), 1.03-0.75(br, 63H). GPC: M_w = 105200; M_n = 20000; polydispersity = 5.26.

OH-HP2: ^{1}H NMR (600MHz, DMSO-d_6, δ): 17.25 (br, 1H), 8.61-8.30 (br, 3H), 8.28-8.13 (br, 3H), 8.01-7.48 (br, 13H), 7.03 (br, 1H), 3.10-2.86 (br, 8H), 2.38-2.01 (br, 18H), 1.03-0.71(br, 63, 114H). . GPC: M_w = 63900; M_n = 23000; polydispersity = 2.78.

OH-HP3: ^{1}H NMR (600MHz, DMSO-d_6, δ): 17.25 (br, 1H), 8.64-8.29 (br, 3H), 8.27-8.06 (br, 3H), 8.00-7.44 (br, 17H), 7.00 (br, 1H), 3.11-2.80 (br, 5H), 2.34-1.99 (br, 8H), 1.01-0.74(br, 63, 38H). . GPC: M_w = 39700; M_n = 18900; polydispersity = 2.10.

OH-HP4: ^{1}H NMR (600MHz, DMSO-d_6, δ): 17.25 (br, 1H), 8.63-8.29 (br, 3H), 8.27-8.04 (br, 5H), 8.01-7.47 (br, 26H), 7.00 (br, 1H), 3.11-2.79 (br, 2H), 2.32-1.99 (br, 10H), 0.99-0.69 (br, 42H). GPC: M_w = 53100; M_n = 18700; polydispersity = 2.84.

OH-LP5: ^{1}H NMR (600MHz, DMSO-d_6, δ): 17.10 (br, 1H), 8.20-8.10 (br, 2H), 7.94-7.47 (br, 12H), 7.01 (br,1H), 2.16-2.00 (br, 4H), 1.36-1.17 (br, 12H), 0.94-0.56 (br, 18H). GPC: M_w = 26900; M_n = 13200; polydispersity = 2.80.

BF$_2$-HP1-4 and **BF$_2$-FLP5.** To a solution of **OH-HP1-4** or **OH-LP5** (90 mg) in CH_2Cl_2 (30 mL), borontrifluoride-ether complex (0.1 g, 0.345 mmol) was added to the reaction mixture. The resulting mixture was stirred at room temperature for 6 h. After reaction, water and CH_2Cl_2 (100 mL) were added, and the organic layer was separated and washed with water three times, dried over Na_2SO_4, and concentrated to dryness. The crude polymers were precipitated from THF into a large excess of hexane. The product was isolated by centrifugation and dried under vacuum. The resulting polymers were obtained as a red powder.

BF$_2$-HP1: ^{1}H NMR (600MHz, DMSO-d_6, δ): 8.60-8.28 (br, 6H), 8.12-7.60 (br, 11H), 7.39 (br, 1H), 3.11-2.92 (br, 6H), 2.31-1.98 (br, 18H), 1.27 (br, 18H), 1.03-0.68 (br, 70H). ^{19}F NMR (564 MHz, $CDCl_3$, δ): -150.65 ($^{10}BF_2$), -150.71 ($^{11}BF_2$). GPC: M_w = 148000; M_n = 18500; polydispersity = 8.01.

BF$_2$-HP2: ^{1}H NMR (600MHz, DMSO-d_6, δ): 8.81-8.28 (br, 6H), 8.03-7.75 (br, 14H), 7.39 (br, 1H), 3.10-2.92 (br, 6H), 2.50-2.09 (br, 16H), 1.27 (br, 13H), 1.04-0.73(br, 54H). ^{19}F NMR (564 MHz, $CDCl_3$, δ): -150.62 ($^{10}BF_2$), -150.68 ($^{11}BF_2$). GPC: M_w = 160600; M_n = 21700; polydispersity = 7.40.

BF$_2$-HP3: ^{1}H NMR (600MHz, DMSO-d_6, δ): 8.64-8.26 (br, 6H), 8.11-7.58 (br, 16H), 7.39 (br, 1H), 3.16-2.81 (br, 5H), 2.34-1.98 (br, 12H), 1.28 (br, 6H), 1.02-0.67 (br, 40H). ^{19}F NMR (564 MHz, $CDCl_3$, δ): -150.60 ($^{10}BF_2$), -150.65 ($^{11}BF_2$). GPC: M_w = 50200; M_n = 18600; polydispersity = 2.69.

BF$_2$-HP4: ^{1}H NMR (600MHz, DMSO-d_6, δ): 8.63-8.23 (br, 6H), 8.11-7.57 (br, 22H), 7.39 (br, 1H), 3.11-2.91 (br, 4H), 2.24-1.98 (br, 10H), 1.29 (br, 3H), 1.02-0.67 (br, 30H). ^{19}F NMR (564 MHz, $CDCl_3$, δ): -150.63 ($^{10}BF_2$), -150.69 ($^{11}BF_2$). GPC: M_w = 31600; M_n = 18700; polydispersity = 1.69.

BF_2-LP5: ^{1}H NMR (600MHz, DMSO-d_6, δ): 8.40-8.25 (br, 2H), 7.97-7.53 (br, 12H), 7.33 (br, 1H), 2.18-2.01 (br, 4H), 1.32-1.17 (br, 12H), 0.94-0.59 (br, 18H). ^{19}F NMR (564 MHz, $CDCl_3$, δ): -150.66 ($^{10}BF_2$), -150.71 ($^{11}BF_2$). GPC: M_w = 21800; M_n = 12100; polydispersity = 1.80.

4. Conclusions

In summary, we have successfully prepared a series of hyperbranched polymers (**BF_2-HP**) containing difluoroboron β-diketonate and truxene units via the Pd(0)-catalyzed Suzuki coupling reaction by an "$A_2 + B_3$" or "$A_2 + B_2 + B_3$" approach. These organoboron-containing polymers exhibited red-shifted emission compared with their uncomplexed counterparts. The optical properties can be tuned by the hyperbranched architectures. In chloroform solution, the emission spectra exhibited significant blue-shift with the increase of linear length in the hyperbranched architecture, whereas a red-shift resulted in the film state, indicating that hyperbranched structure can effectively suppress the aggregation in the solid state. Furthermore, these polymers exhibited high thermal stability, and good solubility in common organic solvents.

Acknowledgements: Financial support by the National Natural Science Foundation of China (21274037 and 21474026), the Natural Science Foundation of Hebei Province (B2016418005), the Youth Foundation of Hebei Educational Committee (QN2014069) and Hebei University construction project for comprehensive strength promotion of Midwest colleges and universities is gratefully acknowledged.

References

[1] Zhang G, Lu J, Sabat M, Fraser CL. Polymorphism and reversible mechanochromic luminescence for solid-state difluoroboron avobenzone. J Am Chem Soc 2010;132:2160-2.

[2] Zhang G, Palmer GM, Dewhirst MW, Fraser CL. A dual-emissive-materials design concept enables tumour hypoxia imaging. Nat Mater 2009;8:747-51.

[3] Nagai A, Kokado K, Nagata Y, Arita M, Chujo Y. Highly intense fluorescent diarylboron diketonate. J Org Chem 2008;73:8605-7.

[4] Liu M, Zhai L, Sun J, Xue P, Gong P, Zhang Z, et al. Multi-color solid-state luminescence of difluoroboron β-diketonate complexes bearing carbazole with mechanofluorochromism and thermofluorochromism. Dyes Pigments 2016;128:271-8.

[5] Ran C, Xu X, Raymond SB, Ferrara BJ, Neal K, Bacskai BJ, et al. Design, synthesis, and testing of difluoroboron-derivatized curcumins as near-infrared probes for in vivo detection of amyloid-β deposits. J Am Chem Soc 2009;131:15257-61.

[6] Zhou Y, Chen YZ, Cao JH, Yang QZ, Wu LZ, Tung CH, et al. Dicyanoboron diketonate dyes: Synthesis, photophysical properties and bioimaging. Dyes Pigments 2015;112:162-9.

[7] Hales J M, Zheng S, Barlow S, Marder SR, Perry JW. Bisdioxaborine polymethines with large third-order nonlinearities for all-optical signal processing. J Am Chem Soc 2006;128:11362-63.

[8] Tanaka K, Chujo Y. Recent progress of optical functional nanomaterials based on organoboron complexes with β-diketonate, ketoiminate and diiminate. NPG Asia Mater 2015;7: e223.

[9] Kinoshita Y, Kitagawa Y, Tamiaki H. Enhancement of Light Absorption Ability of Synthetic Chlorophyll Derivatives by Conjugation with a Difluoroboron Diketonate Group. Chem Eur J 2016;22:9996-10001.

[10] Poon CT, Lam WH, Wong HL, Yam VWW. A versatile photochromic dithienylethene-containing β-diketonate ligand: Near-infrared photochromic behavior and photoswitchable luminescence properties upon incorporation of a boron (III) center. J Am Chem Soc 2010;132:13992-3.

[11] Butler T, Morris WA, Samonina-Kosicka J, Fraser CL. Mechanochromic luminescence and aggregation induced emission for a metal-free β-diketone. Chem Commun 2015;51:3359-62.

[12] Morris WA, Liu T, Fraser CL. Mechanochromic luminescence of halide-substituted difluoroboron β-diketonate dyes. J Mater Chem C 2015;3:352-63.

[13] Samonina-Kosicka J, Weitzel DH, Hofmann CL, Hendargo H, Hanna G, Dewhirst MW, et al. Luminescent difluoroboron β-Diketonate PEG-PLA oxygen nanosensors for tumor imaging. Macromol Rapid Commun 2015;36:694-9.

[14] Butler T, Morris WA, Samonina-Kosicka J, Fraser CL. Mechanochromic luminescence and aggregation induced emission of dinaphthoylmethane β-diketones and their boronated counterparts. ACS Appl Mater Interfaces 2016;8:1242-51.

[15] Zhang G, St Clair TL, Fraser CL. Synthesis and fluorescent properties of difluoroboron dibenzoylmethane polycaprolactone. Macromolecules 2009;42:3092-3097.

[16] Tanaka K, Tamashima K, Nagai A, Okawa T, Chujo Y. Facile modulation of optical properties of diketonate-containing polymers by regulating complexation ratios with boron. Macromolecules 2013;46:2969-75.

[17] Wu W, Tang R, Li Q, Li Z. Functional hyperbranched polymers with advanced optical, electrical and magnetic properties. Chem Soc Rev 2015;44:3997-4022.

[18] Tan S, Ma H, Liu W, Zhao H, Wu Y, Ba X. Synthesis and characterization of conjugated polymers containing bifluorenylidenes units. Chem J Chinese U 2014;6:1355-62.

[19] Sun J, Wang H, Yang T, Zhang X, Li J, Zhang T, et al. Design, synthesis and properties of triple-color hyperbranched polymers derived from poly (9,9-dioctylfluorene) with phosphorescent core tris(1-phenylisoquinoline) iridium (Ⅲ). Dyes Pigments 2016;125:339-47.

[20] Jackson NE, Kohlstedt KL, Savoie BM, Olvera De La Cruz M, Schatz GC, Chen LX, et al. Conformational order in aggregates of conjugated polymers. J Am Chem Soc 2015;137:6254-62.

[21] Wu JS, Cheng SW, Cheng YJ, Hsu CS. Donor–acceptor conjugated polymers based on multifused ladder-type arenes for organic solar cells. Chem Soc Rev 2015;44:1113-54.

[22] Guo X, Baumgarten M, Müllen K. Designing π-conjugated polymers for organic electronics. Prog Polym Sci 2013;38:1832-908.

[23] Yokozawa T, Yokoyama A. Chain-growth condensation polymerization for the synthesis of well-defined condensation polymers and π-conjugated polymers. Chem Rev 2009;109:5595-619.

[24] Jiang H, Taranekar P, Reynolds JR, Schanze KS. Conjugated polyelectrolytes: synthesis, photophysics, and applications. Angew Chem Int Ed 2009;48:4300-16.

[25] Irfan M, Seiler M. Encapsulation using hyperbranched polymers: from research and technologies to emerging applications. Ind Eng Chem Res 2010;49:1169-96.

[26] Tolosa J, Kub C, Bunz UH. Hyperbranched: A universal conjugated polymer platform. Angew Chem Int Ed 2009;48:4610-2.

[27] Khotina IA, Lepnev LS, Burenkova NS, Valetsky PM, Vitukhnovsky AG. Phenylene dendrimers and novel hyperbranched polyphenylenes as light emissive materials for blue OLEDs. J Lumin 2004;110:232-8.

[28] Kwak G, Takagi A, Fujiki M, Masuda T. Facile preparation of transparent, homogeneous, fluorescent gel film based on σ-π-conjugated, hyperbranched polymer with siloxane linkages by means of hydrosilylation and aerial oxidation. Chem Mater 2004;16:781-5.

[29] Ding D, Wang G, Liu J, Li K, Pu KY, Hu Y, et al. Hyperbranched conjugated polyelectrolyte for dual-modality fluorescence and magnetic resonance cancer imaging. Small 2012;8:3523-30.

[30] Rubio-Magnieto J, Thomas A, Richeter S, Mehdi A, Dubois P, Lazzaroni R, et al. Chirality in DNA–π-conjugated polymer supramolecular structures: insights into the self-assembly. Chem Commun 2013;49:5483-5.

[31] Wu Y, Hao X, Wu J, Jin J, Ba X. Pure blue-light-emitting materials: hyperbranched ladder-type poly(p-phenylene)s containing truxene units. Macromolecules 2010;43(2):731-738.

[32] Tan S, Ma H, Liu W, Zhao H, Wu Y, Ba X. Synthesis and characterization of conjugated polymers containing bifluorenylidenes units. Chem J Chinese U 2014;6:1355-62.

[33] Chen H, He M, Pei J, Liu B. End-group analysis of blue light-emitting polymers using matrix-assisted laser desorption/ionization time-of-flight mass spectrometry. Anal Chem 2002;74:6252-8.

[34] Kanibolotsky AL, Berridge R, Skabara PJ, Perepichka IF, Bradley DD, Koeberg M. Synthesis and properties of monodisperse oligofluorene-functionalized truxenes: highly fluorescent star-shaped architectures. J Am Chem Soc 2004;126:13695-702.

[35] Pérez P, Toro-Labbé A. Characterization of keto-enol tautomerism of acetyl derivatives from the analysis of energy, chemical potential, and hardness. J Phys Chem A 2000;104:1557-62.

[36] He T, Gao Y, Chen R, Ma L, Rajwar D, Wang Y, et al. Multiphoton harvesting in an angular carbazole-containing Zn(II)-coordinated random copolymer mediated by twisted intramolecular charge transfer state. Macromolecules 2014;47:1316-24.

[37] Zhang GF, Aldred MP, Gong WL, Li C, Zhu MQ. Utilising tetraphenylethene as a dual activator for intramolecular charge transfer and aggregation induced emission. Chem Commun 2012;48:7711-3.

[38] Li J, Bo Z. “AB_2+AB” approach to hyperbranched polymers used as polymer blue light emitting materials. Macromolecules 2004;37:2013-5.

[39] Chen P, Marshall AS, Chi SH, Yin X, Perry JW, Jäkle F. Luminescent quadrupolar borazine oligomers: synthesis, photophysics, and two-photon absorption properties. Chem Eur J 2015;21:18237-47.

[40] Yang Z, Qin W, Lam JW, Chen S, Sung HH, Williams ID, et al. Fluorescent pH sensor constructed from a heteroatom-containing luminogen with tunable AIE and ICT characteristics. Chem Sci 2013;4:3725-30.

[41] Cao C, Liu X, Qiao Q, Zhao M, Yin W, Mao D, et al. A twisted-intramolecular-charge-transfer (TICT) based ratiometric fluorescent thermometer with a mega-Stokes shift and a positive temperature coefficient. Chem Commun 2014;50:15811-14.

[42] Zhang GF, Aldred MP, Gong WL, Li C, Zhu MQ. Utilising tetraphenylethene as a dual activator for intramolecular charge transfer and aggregation induced emission. Chem Commun 2012;48:7711-3.

[43] De Luca G, Liscio A, Maccagnani P, Nolde F, Palermo V, Müllen K, Samori P. Nucleation-governed reversible self-assembly of an organic semiconductor at surfaces: long-range mass transport forming giant functional fibers. Adv Funct Mater 2007;17:3791-8.

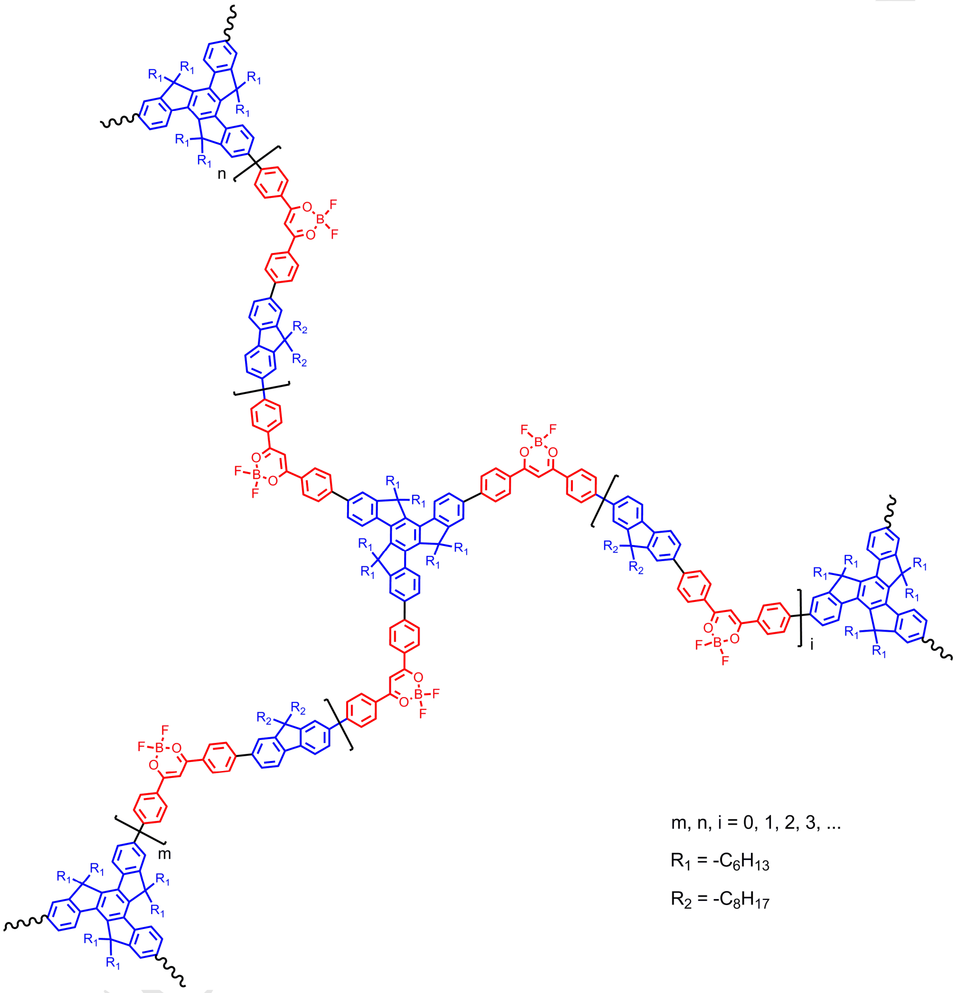

m, n, i = 0, 1, 2, 3, ...

R_1 = -C_6H_{13}

R_2 = -C_8H_{17}

Scheme 1. Chemical structures of the hyperbranched polymers **BF$_2$-HP(1-4)**.

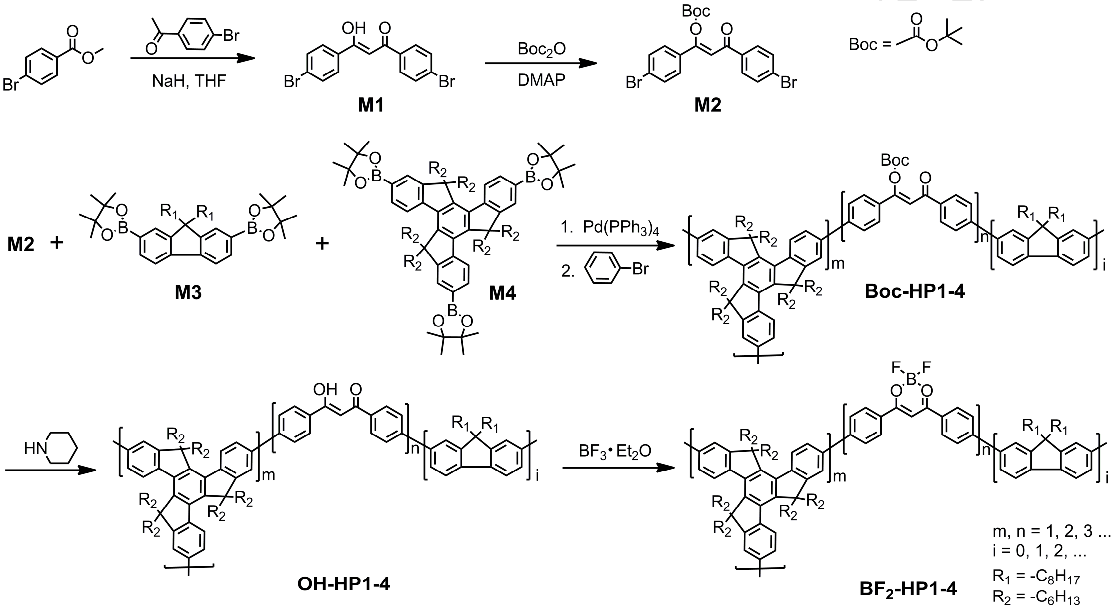

Scheme 2. Synthesis of the monomers and hyperbranched polymers **BF$_2$-HP1-4**.

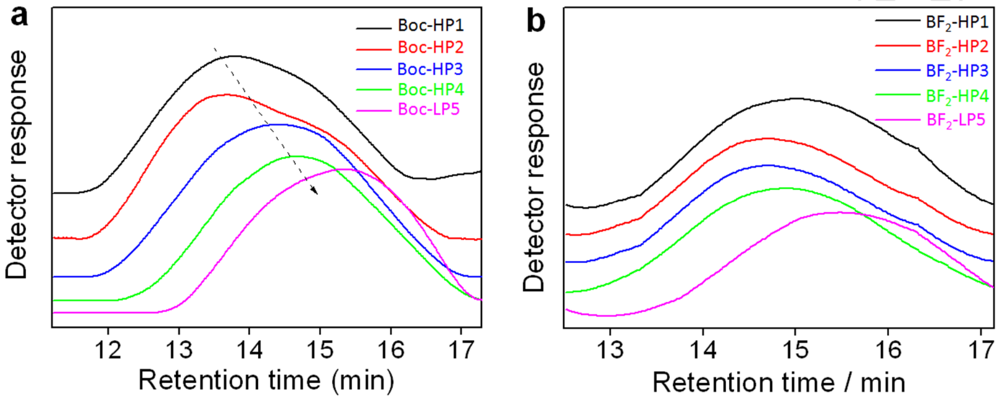

Fig. 1. GPC elution traces of polymers (a) **Boc-HP1-4** and **Boc-LP5**, (b) **BF_2-HP1-4** and **BF_2-LP5**.

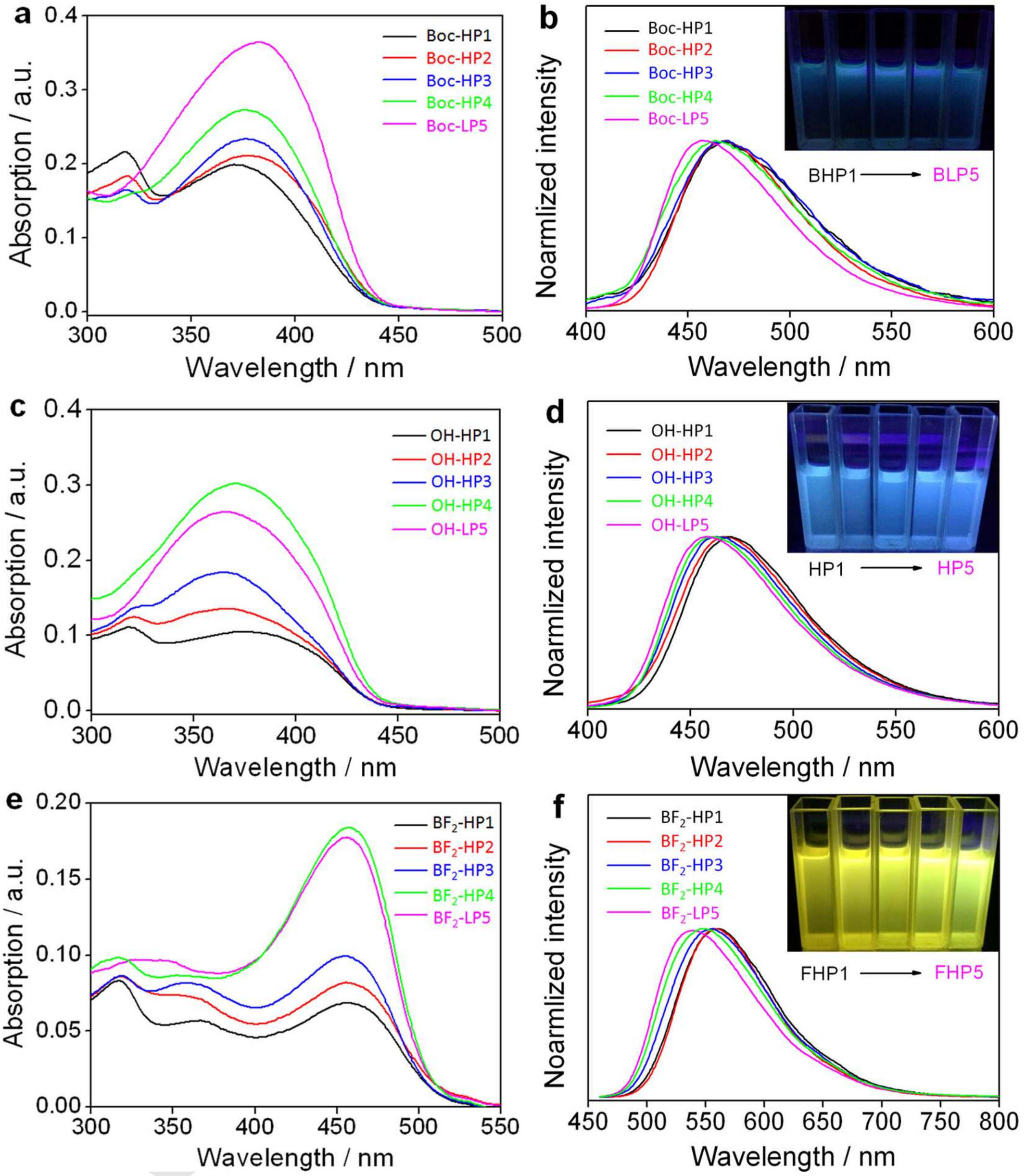

Fig. 2. UV-vis absorption and PL spectra of (a), (b) **Boc-HP1-4** and **Boc-LP5**; (c), (d) **OH-HP1-4** and **OH-LP5**; (e), (f) **BF$_2$-HP1-4** and **BF$_2$-LP5** in chloroform.

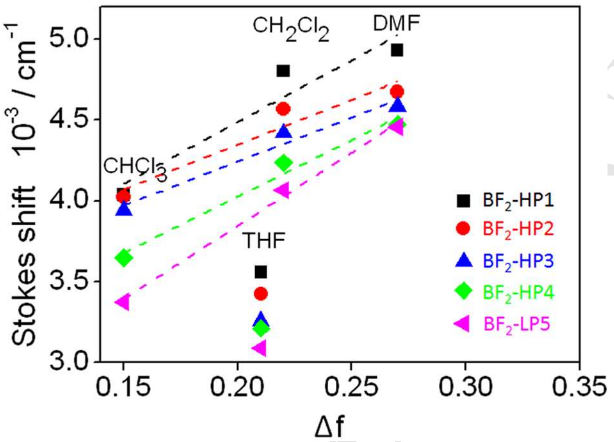

Fig. 3. Lippert−Mataga plots of the polymers obtained from the data in Table 2. Δf is the orientational polarisability of solvent.

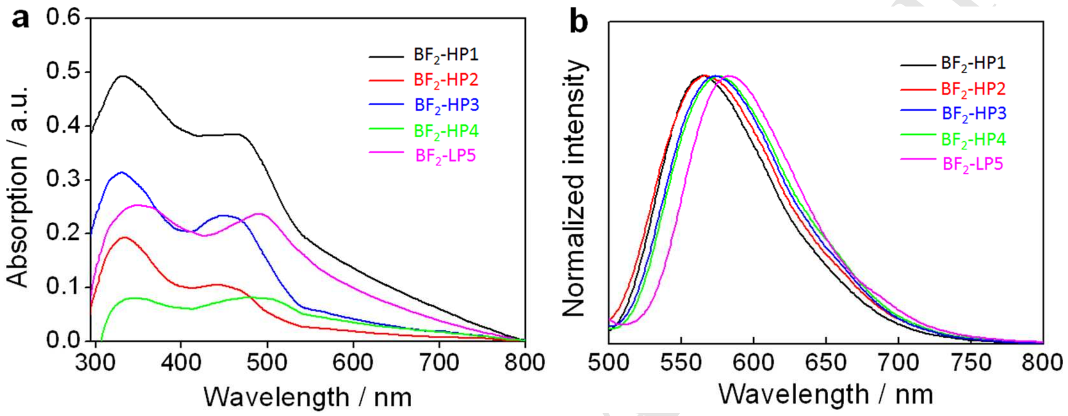

Fig. 4. UV-vis absorption (a) and PL spectra (b) of polymers **BF$_2$-HP1-4** and **BF$_2$-LP5** in film.

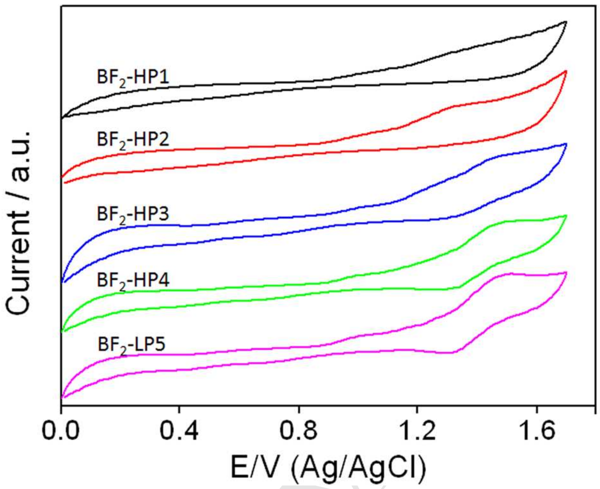

Fig. 5. Cyclic voltammograms of **BF$_2$-HP1-4** and **BF$_2$-LP5** in anhydrous methylene chloride at a scan rate of 30 mV s^{-1}.

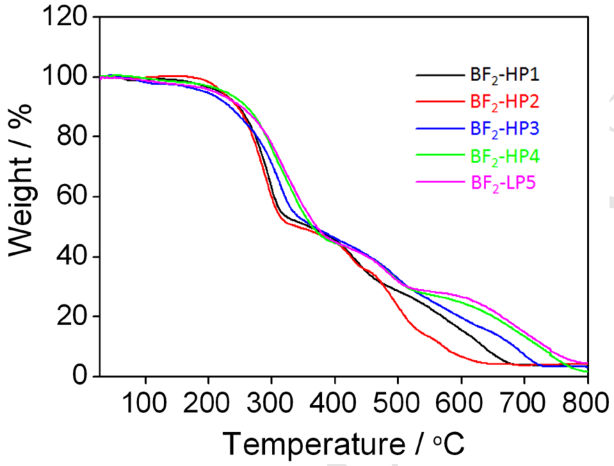

Fig. 6. TGA traces of **BF_2-HP1-4** and **BF_2-LP5**.

Table 1. The polymer weight of synthesized polymers.

polymers	M_n	M_w	M_w/M_n	yield (%)	T_d (^oC)
Boc-HP1	28300	56300	1.99	44	-
Boc-HP2	28100	69400	2.47	63	-
Boc-HP3	26700	60800	2.28	62	-
Boc-HP4	21200	44100	2.08	62	-
Boc-LP5	15100	30200	2.00	53	-
BF_2-HP1	18500	148100	8.01	41	221
BF_2-HP2	21700	160600	7.40	57	223
BF_2-HP3	18600	50200	2.70	59	201
BF_2-HP4	18700	31600	1.69	58	226
BF_2-LP5	12100	21800	1.80	50	210

Table 2. Photophysical properties of **BF$_2$-HP1-4** and **BF$_2$-LP5** in various solvents.

Compd	$CHCl_3$			THF			CH_2Cl_2			DMF		
	$\lambda_{PL,max}$ (nm)	Stokes shift (cm^{-1})	$\Phi_{PL}{}^{a}$	$\lambda_{PL,max}$ (nm)	Stokes shift (cm^{-1})	$\Phi_{PL}{}^{a}$	$\lambda_{PL,max}$ (nm)	Stokes shift (cm^{-1})	$\Phi_{PL}{}^{a}$	λ_{PLmax} (nm)	Stokes shift (cm^{-1})	$\Phi_{PL}{}^{a}$
BF$_2$-HP1	562	4040	0.27	535	3580	0.18	584	4903	0.10	585	4932	0.036
BF$_2$-HP2	560	4025	0.29	534	3446	0.19	581	4670	0.13	586	4674	0.048
BF$_2$-HP3	556	3944	0.33	532	3278	0.21	576	4521	0.15	591	4585	0.053
BF$_2$-HP4	547	3649	0.35	530	3234	0.30	570	4338	0.21	592	4476	0.054
BF$_2$-LP5	539	3377	0.35	528	3110	0.33	563	4168	0.23	593	4459	0.069

[a] using *N*,*N′*-bis(1-ethylpropyl)-3,4,9,10-perylene-bis(dicarboximide) as a reference standard [43].

Table 3. Photophysical properties of **BF$_2$-HP1-4** and **BF$_2$-LP5** in chloroform and film.

Polymers	$\lambda_{\text{abs, max, solution}}$ (nm)	$\lambda_{\text{abs, max, film}}$ (nm)	$\lambda_{\text{PL, max, solution}}$ (nm)	$\lambda_{\text{PL, max, film}}$ (nm)	$\Phi_{\text{PL, film}}$ [a]
BF$_2$-HP1	458	440	562	565	0.018
BF$_2$-HP2	457	441	560	567	0.037
BF$_2$-HP3	456	449	556	573	0.040
BF$_2$-HP4	456	486	547	576	0.025
BF$_2$-LP5	456	490	539	584	0.020

[a] Absolute quantum yield.

Table 4. HOMO and LUMO energies and band gap data of **BF$_2$-HP1-4** and **BF$_2$-LP5**.

polymers	**BF$_2$-HP1**	**BF$_2$-HP2**	**BF$_2$-HP3**	**BF$_2$-HP4**	**BF$_2$-LP5**
HOMO (ev)	-5.42	-5.49	-5.53	-5.61	-5.63
LOMO (ev)	-3.02	-3.08	-3.11	-3.17	-3.19
band gap (ev)	2.40	2.41	2.43	2.45	2.46

Highlights:

- Hyperbranched polymers containing difluoroboron-diketonate units were synthesized.
- These polymers exhibited obvious red-shifts in UV-vis absorption and emission.
- The tunable hyperbranched architectures resulted in diverse optical properties.
- The hyperbranched architectures could suppress the aggregation more effectively.
- These polymers showed good thermal stability and solubility.